Overview of ER-2 Radar Observations, WRF, and Radar Retrievals from IPHEX and OLYMPEX

Gerald Heymsfield[1], Stephen D. Nicholls[1,2], and Mircea Grecu[1,3]
NASA-Goddard Space Flight Center[1], Joint Center for Earth Systems Technology[2], Morgan State University[3]

Objectives

- Cross-evaluate microphysical characteristics and physical properties of orographic precipitation from GPM algorithm retrievals, GPM GV, and WRF
- Quantify how terrain modifies and impacts orographic precipitation properties
- Assess the capability of WRF and an aircraft-based experimental radar retrieval for ice to characterize cloud tops and associated particle properties
- Quantify particle growth and drop size distributions within the GPM ground clutter zone
- Create characteristic precipitation processes in GPM ground clutter regions

Datasets

1. **Weather Research and Forecasting model (WRF)**
   - 4-model domains (27, 9, 3,1 km)
   - ECMWF interim input
   - Goddard 4-ice
   - Initialized 24-hour before ER-2
   - 15 minute output interval
   - Satellite data simulator (G-SDSU)
2. **Aircraft and Surface Obs.**
   - Ka-band – HIWRAP (35.5 GHz)
   - Ku-band – HIWRAP (13.6 GHz)
   - W-band – CRS (94 GHz)
   - X-band – EXRAD (9.4 GHz)
   - Radiometers
     - AMPR (10-85 GHz)
     - CoSMIR (89-103 GHz)
   - Polarmetric radars
     - NPOL, D3R, WSR-88D
   - Surface rainfall
     - Gauges, Pluvio, MRR
3. **Experimental Radar Retrieval for Ice (ERRI; Grecu, 2018*)**
   - Proposed for inclusion in GPM
   - Applied to ER-2 radar data (Ka-, Ku-, W-bands)
   - Provided data
     - Drop size distribution
     - Ice water content
     - Attenuation corrected radar (under development)

IPHEX (2014/06/12)

Case description: Post frontal passage with widely scattered convection over NC mountains

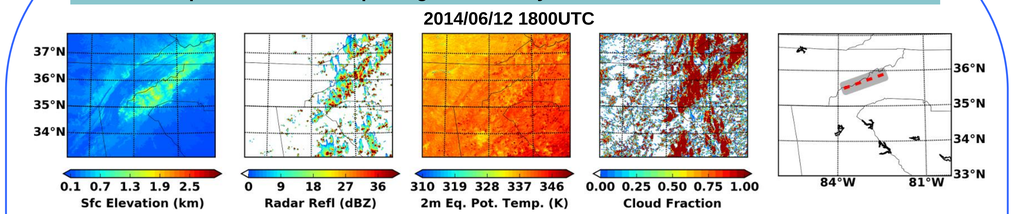

Fig. 1: June 2014 case overview showing WRF-derived surface elevation (km), radar reflectivity (dBZ), 2m equivalent potential temperature (K), total cloud fraction, and the approximate track of the ER-2 aircraft near 1800 UTC on 12 June 2014.

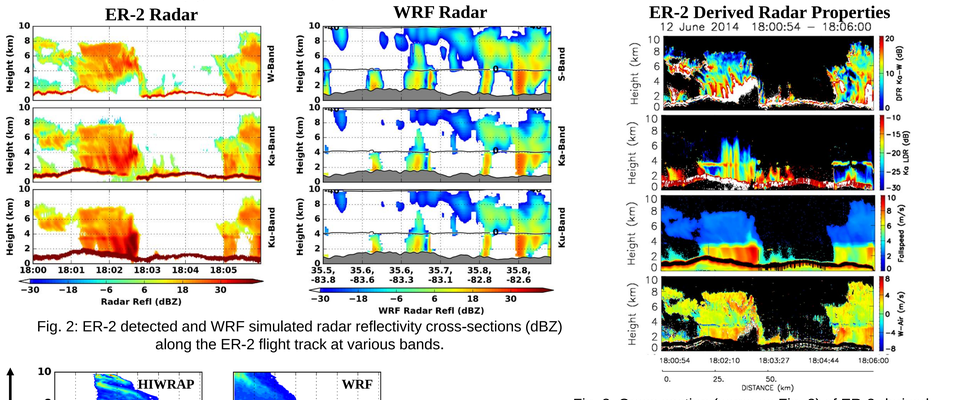

Fig. 2: ER-2 detected and WRF simulated radar reflectivity cross-sections (dBZ) along the ER-2 flight track at various bands.

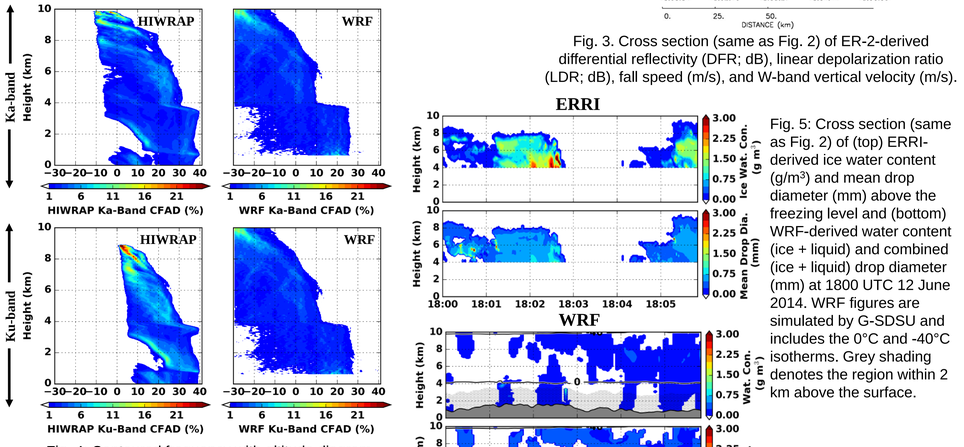

Fig. 4: Contoured frequency with altitude diagram (CFAD) along ER-2 flight track near 1800 UTC on 12 June 2014 at (top) Ka- and (bottom) Ku-bands derived from HIWRAP and WRF.

Fig. 3. Cross section (same as Fig. 2) of ER-2-derived differential reflectivity (DFR; dB), linear depolarization ratio (LDR; dB), fall speed (m/s), and W-band vertical velocity (m/s).

Fig. 5: Cross section (same as Fig. 2) of (top) ERRI-derived ice water content (g/m^3) and mean drop diameter (mm) above the freezing level and (bottom) WRF-derived water content (ice + liquid) and combined (ice + liquid) drop diameter (mm) at 1800 UTC 12 June 2014. WRF figures are simulated by G-SDSU and includes the 0°C and -40°C isotherms. Grey shading denotes the region within 2 km above the surface.

OLYMPEX (2015/12/05)

Case description: Broad frontal cloud system with strong wind shear

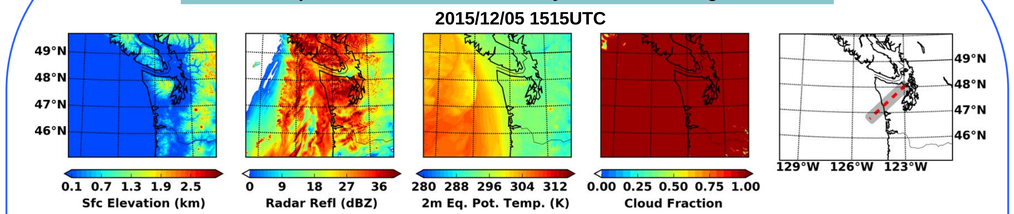

Fig. 6: December 2015 case overview showing WRF-derived surface elevation (km), radar reflectivity (dBZ), 2m equivalent potential temperature (K), total cloud fraction, and the approximate ER-2 flight track near 1515UTC on 05 Dec. 2015.

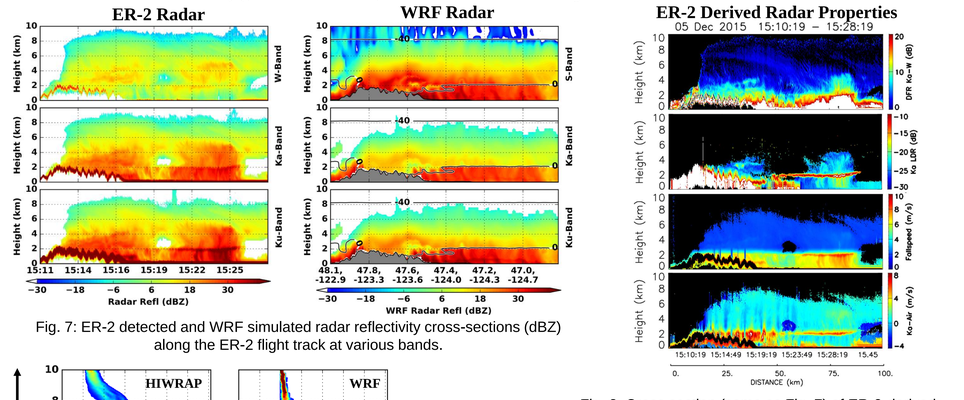

Fig. 7: ER-2 detected and WRF simulated radar reflectivity cross-sections (dBZ) along the ER-2 flight track at various bands.

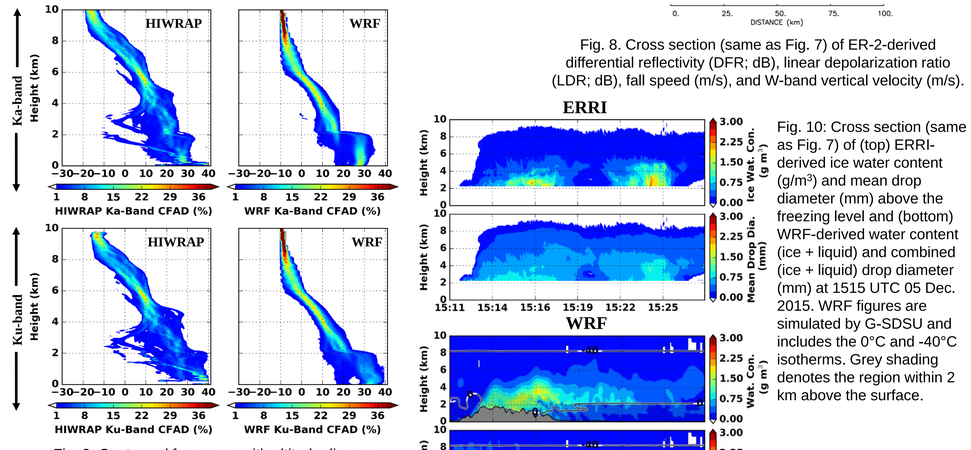

Fig. 9: Contoured frequency with altitude diagram (CFAD) along ER-2 flight track path near 1515 UTC on 05 Dec. 2015 at (top) Ka- and (bottom) Ku-bands derived from HIWRAP and WRF.

Fig. 8. Cross section (same as Fig. 7) of ER-2-derived differential reflectivity (DFR; dB), linear depolarization ratio (LDR; dB), fall speed (m/s), and W-band vertical velocity (m/s).

Fig. 10: Cross section (same as Fig. 7) of (top) ERRI-derived ice water content (g/m^3) and mean drop diameter (mm) above the freezing level and (bottom) WRF-derived water content (ice + liquid) and combined (ice + liquid) drop diameter (mm) at 1515 UTC 05 Dec. 2015. WRF figures are simulated by G-SDSU and includes the 0°C and -40°C isotherms. Grey shading denotes the region within 2 km above the surface.

Discussion of Figures

- Two pilot cases illustrate vastly different background environmental drivers for storm generation (convective instability vs large-scale ascent).
  - IPHEX: Widely scattered convection, small baroclinicity, higher potential instability (high Θ_e), focused generation on orography (Fig. 1)
  - OLYMPEX: Large precipitation coverage, strong baroclinicity, lower potential instability (low Θ_e), orographic enhancement (Fig. 6)
- Figures 2-5 and 6-10 show retrieved or simulated radar and precipitation properties obtained from the ER-2 aircraft (HIWRAP, CRS), the ERRI (assimilates ER-2 radar data), and WRF model forecasts (1-km resolution, no data assimilation or grid nudging).
- WRF radar cross-sections (Figs. 2 and 7) and CFADs (Figs. 4 and 9) demonstrate better forecast skill for OLYMPEX than IPHEX because the frontal lift mechanisms could be adequately resolved at the model resolution, yet localized convection occurs at near or sub-grid scale.
- Additional environmental properties obtained from the ER-2 (i.e., Figs. 3 and 8) show vertical velocity values that can exceed that produced by WRF (not shown) by up to 5 m/s (IPHEX case) and graupel production at higher altitudes. This was less of an issue for OLYMPEX.
- Particle properties (Figs. 5 and 10) are more realistic in OLYMPEX than IPHEX, yet WRF characterizes the freezing level accurately in both.
- In situations of improved forecast skill (OLYMPEX), WRF reasonably simulates water content, but tends to over estimate droplet size.
  - This may change when utilizing other microphysics schemes or "light" grid nudging to help reduce spatio-temporal errors.

***Grecu, M., L. Tian, G. Heymsfield, A. Tokay, W.S. Olson, A.J. Heymsfield, and A. Bansemer, 2018: Non-parametric methodology to estimate precipitating ice from multiple frequency radar reflectivity observations, *J. Appl. Meteor. Clim.*, in-press.**

Summary

- This overview illustrates the potential capabilities of a combined ER-2, ERRI, and WRF approach to representing precipitating systems and hydrometeor particle properties in orographic regions.
- ERRI utilizes ER-2 radar (Ka-, Ku-, and W-bands), but (for now) focuses exclusively on the ice phase only and aims to be incorporated into the future GPM combined algorithm.
- ERRI provides useful added value to ER-2 radar products via the inclusion of ice-phase hydrometeor particle properties.
- The comparatively coarse grid spacing of WRF (1-km) yields closer correspondence to ER-2 for the synoptically-forced OLYMPEX event as compared to the locally-instability focused IPHEX case.
- Simulation errors may potentially be reduced via the application of more complex microphysics schemes (i.e., Morrison, P-3) or "light" grid nudging (i.e., 12-hour interval), but this requires further investigation.
- Despite differences in forecast skill between the cases, WRF does realistically capture the freezing level in both cases.
- Pilot WRF simulations tend bias high (radar reflectivity and hydrometeor particle size) relative to aircraft retrievals, which could be used to inform potential improvements needed to address these short comings in WRF.